

Medium modifications of nucleon electromagnetic form factors

T. Horikawa

Department of Physics, School of Science, Tokai University
Hiratsuka-shi, Kanagawa 259-1292, Japan

W. Bentz *

Department of Physics, School of Science, Tokai University
Hiratsuka-shi, Kanagawa 259-1292, Japan

Abstract

We use the Nambu-Jona-Lasinio model as an effective quark theory to investigate the medium modifications of the nucleon electromagnetic form factors. By using the equation of state of nuclear matter derived in this model, we discuss the results based on the naive quark - scalar diquark picture, the effects of finite diquark size, and the meson cloud around the constituent quarks. We apply this description to the longitudinal response function for quasielastic electron scattering. RPA correlations, based on the nucleon-nucleon interaction derived in the same model, are also taken into account in the calculation of the response function.

PACS numbers: 12.39.Fe; 12.39.Ki; 13.40.Gp; 14.20.Dh; 14.65.-q

Keywords: Chiral quark theories, Nucleon form factors, Medium modifications

*Correspondence to: W. Bentz, E-mail: bentz@keyaki.cc.u-tokai.ac.jp

1 Introduction

The structure of the nucleon and its modifications in the nuclear medium is a very active field of experimental and theoretical research. The basic quantities, which reflect the charge and current distributions in the nucleon, are the electromagnetic form factors [1], which are currently investigated in elastic electron- nucleon scattering experiments from intermediate to very high energies [2]. The knowledge of the nucleon form factors is also inevitable to understand the electromagnetic structure of nuclei. Electron-nucleus scattering experiments under quasielastic kinematic conditions, like the measurement of inclusive response functions in the intermediate energy region [3, 4] and recent measurements of polarization transfer in semi-exclusive knock-out processes [5], are ideal places to study the form factors of a nucleon bound in the nuclear medium. Because the structure of the quark core and the surrounding meson cloud may be different for a bound nucleon and a free nucleon, one expects medium modifications of the nucleon form factors[6], and the exploration of these effects is an important subject at current electron accelerator facilities [7].

On the theoretical side, effective quark theories are the ideal tools to describe the electromagnetic form factors of the nucleon. Much progress for the case of the free nucleon has been made in Faddeev type descriptions based on the Schwinger-Dyson method [8]. An important point which still has to be implemented in these calculations is the role of the pion cloud around the nucleon, and the recently developed method of chiral extrapolations of lattice results [9] provides important hints. On the other hand, the calculation of form factors at finite nucleon density requires also a description of the equation of state of the many-nucleon system, and here progress has been made by using the Nambu-Jona-Lasinio (NJL) model [10] as an effective

quark theory: Recent works have shown how to account for the saturation properties of nuclear matter in this model [11], and when combined with the quark-diquark description of the single nucleon[12] this provides a successful description of both nucleon and nuclear structure functions for deep inelastic scattering [13, 14] ¹.

The purpose of this paper is to discuss the results for the nucleon form factors obtained in the simple quark-scalar diquark description of the nucleon at finite density in the NJL model. We have to note from the beginning that this can only be a first step toward a realistic description, because it is known that axial vector diquarks are important for spin-dependent quantities[17, 14], and the pion cloud is important for magnetic moments and the size of the nucleon[9, 18]. While the axial diquarks could be included in a further step like it was done for the structure functions[14], a reliable description of pion cloud effects makes it necessary to go beyond the standard ladder approximation scheme. However, like the simple quark-scalar diquark model of Ref.[13] served as a basis for the more elaborate description of structure functions [14], it will also be the basis of a more realistic description of form factors including axial diquarks and the pion cloud. To provide this basis is the main intention of the present paper.

In Sect. 2 we will briefly review the model for the nucleon and the nuclear matter equation of state. Sect. 3 is devoted to the nucleon form factors at finite density, and in Sect.4 we discuss the numerical results. As an application, we discuss the response function for quasielastic electron scattering in Sect.5. For this purpose we will also elucidate the nucleon-nucleon interaction in our model in order to include the correlations within the relativistic RPA. A summary will be presented in Sect. 6.

¹Recently the model has been extended to describe the equation of state at high densities[15, 16].

2 The model

In this work, we use the NJL model as an effective quark theory to describe the nucleon as a quark-diquark bound state, and nuclear matter (NM) in the mean field approximation. The details are explained in Refs. [11, 15], and here we will only briefly summarize those points which will be needed for our calculations.

The NJL model is characterized by a chirally symmetric 4-fermi interaction between the quarks[19]. Any such interaction can be Fierz symmetrized and decomposed into various $q\bar{q}$ channels [20]. Writing out explicitly only those channels which are relevant for our present discussion, we have

$$\mathcal{L} = \bar{\psi} (i\not{\partial} - m) \psi + G_{\pi} \left((\bar{\psi}\psi)^2 - (\bar{\psi}(\gamma_5 \boldsymbol{\tau})\psi)^2 \right) - G_{\omega} (\bar{\psi}\gamma^{\mu}\psi)^2 + \dots \quad (2.1)$$

where m is the current quark mass. In a mean field description of the isospin symmetric nuclear matter ground state $|\rho\rangle$, the Lagrangian can be expressed as

$$\mathcal{L} = \bar{\psi} (i\not{\partial} - M - \not{V}) \psi - \frac{(M - m)^2}{4G_{\pi}} + \frac{V_{\mu}V^{\mu}}{4G_{\omega}} + \mathcal{L}_I, \quad (2.2)$$

where $M = m - 2G_{\pi}\langle\rho|\bar{\psi}\psi|\rho\rangle$ and $V^{\mu} = 2G_{\omega}\langle\rho|\bar{\psi}\gamma^{\mu}\psi|\rho\rangle$, and \mathcal{L}_I is the normal ordered interaction Lagrangian. The effect of the mean scalar field is thus included in the density-dependent constituent quark mass M , and the effect of the mean vector field is to shift the quark momentum according to $p^{\mu} = p_Q^{\mu} + V^{\mu}$, where p_Q^{μ} is the kinetic momentum. The propagator of the constituent quark therefore has the following dependence on the mean vector field ²: $\tilde{S}(k) = S(k_Q)$.

²In this section, Green functions in the presence of the mean vector field are denoted by a tilde, and those without the vector field have no tilde. In the loop integrals for the electromagnetic form factors in Sect.3, however, it is always possible to eliminate the vector field by a shift of the integration variable, and therefore the tilde-Green functions do not appear in later sections.

One can use a further Fierz transformation to decompose \mathcal{L}_I into a sum of qq channel interaction terms [20]. For our purposes we need only the interaction in the scalar diquark ($J^\pi = 0^+, T = 0$, color $\bar{3}$) channel:

$$\mathcal{L}_{I,s} = G_s \left(\bar{\psi} (\gamma_5 C) \tau_2 \beta^A \bar{\psi}^T \right) \left(\psi^T (C^{-1} \gamma_5) \tau_2 \beta^A \psi \right), \quad (2.3)$$

where $\beta^A = \sqrt{3/2} \lambda^A$ ($A = 2, 5, 7$) are the color $\bar{3}$ matrices and $C = i\gamma_2\gamma_0$. The coupling constant G_s will be determined so as to reproduce the free nucleon mass.

The reduced t-matrix in the scalar diquark channel is given by [11]

$$\tilde{\tau}_s(q) = \frac{4iG_s}{1 + 2G_s\tilde{\Pi}_s(q)} = \tau_s(q_D) \quad (2.4)$$

with the scalar qq bubble graph

$$\tilde{\Pi}_s(q) = 6i \int \frac{d^4k}{(2\pi)^4} \text{tr}_D [\gamma_5 S(k) \gamma_5 S(-(q-k))] = \Pi_s(q_D). \quad (2.5)$$

Here $q_D^\mu = q^\mu - 2V^\mu$ is the kinetic momentum of the diquark.

The relativistic Faddeev equation in the NJL model can be solved numerically for the free nucleon[20], but here we restrict ourselves to the static approximation[21], where the momentum dependence of the quark exchange kernel is neglected. The solution for the quark-diquark t-matrix then takes the simple analytic form

$$\tilde{T}_N(p) = \frac{3}{M} \frac{1}{1 + \frac{3}{M}\tilde{\Pi}_N(p)} = T_N(p_N), \quad (2.6)$$

with the quark-diquark bubble graph given by

$$\tilde{\Pi}_N(p) = - \int \frac{d^4k}{(2\pi)^4} \tilde{S}(k) \tilde{\tau}_s(p-k) = \Pi_N(p_N), \quad (2.7)$$

where $p_N^\mu = p^\mu - 3V^\mu$ is the kinetic momentum of the nucleon. The nucleon mass M_N is defined as the pole of (2.6) at $p_N = M_N$, and the positive energy

spectrum has the form $p_0 = \epsilon_p \equiv E_{Np} + 3V_0$ with $E_{Np} = \sqrt{M_N^2 + \mathbf{p}^2}$. The nucleon vertex function in the non-covariant normalization is defined by the pole behavior of the quark-diquark t-matrix:

$$T_N(p) \rightarrow \frac{\Gamma_N(p) \bar{\Gamma}_N(p)}{p_0 - \epsilon_p} \quad \text{as } p_0 \rightarrow \epsilon_p. \quad (2.8)$$

From this definition and Eq.(2.6) one obtains

$$\Gamma_N(p) = \sqrt{-Z_N \frac{M_N}{E_{Np}}} u_N(p_N), \quad (2.9)$$

where u_N is a free Dirac spinor for mass M_N normalized as $\bar{u}_N u_N = 1$. The normalization factor Z_N is easily obtained from this definition and will be given in Eq.(2.14) below. We note that with this normalization the vertex function satisfies the relation

$$\bar{\Gamma}_N(p) \left(\frac{\partial \Pi_N(p)}{\partial p_\mu} \right) \Gamma_N(p) = \frac{p^\mu}{E_{Np}} \quad (2.10)$$

In the numerical calculations of this paper, we will approximate the quantity τ_s by a “contact+pole” form:

$$\tau_s(q) \rightarrow 4iG_s - \frac{i g_s}{q^2 - M_s^2} \equiv 4iG_s - i g_s \Delta_{Fs}(q). \quad (2.11)$$

Here $\Delta_{Fs}(q)$ is the Feynman propagator for a scalar particle of mass M_s , which is defined as the pole of τ_s of Eq.(2.4). The residue at the pole (g_s) will be given in Eq. (2.13) below.

In the calculation of the nucleon form factors, we will also consider the effects of the pion cloud around the constituent quarks. In this case, the propagator $S(p)$ of the quark involves an additional self energy correction from the pion cloud (Σ_Q). Here we will use a simple pole approximation for $S(p)$:

$$S(p) = Z_Q S_F(p), \quad Z_Q^{-1} = 1 - \left(\frac{\partial \Sigma_Q}{\partial \not{p}} \right)_{\not{p}=M}, \quad (2.12)$$

where S_F is the Feynman propagator of a constituent quark with mass M . In this approximation, the pion effects can be renormalized by $\psi \rightarrow \sqrt{Z_Q}\psi$ and a redefinition of the four fermi coupling constants $G_\alpha \rightarrow G_\alpha/Z_Q^2$, see Ref.([12]). For the calculation of the form factors, however, we will keep the factor Z_Q explicitly for clarity ³. Introducing (2.12) and (2.11) into the expressions (2.5) and (2.7) for the bubble graphs shows that the diquark and nucleon normalization factors can be written as

$$g_s^{-1} = \frac{1}{2} \left(-\frac{\partial \Pi_s(q)}{\partial q^2} \right)_{q^2=M_s^2} = \frac{1}{2} Z_Q^2 \left(-\frac{\partial \hat{\Pi}_s(q)}{\partial q^2} \right)_{q^2=M_s^2} \equiv Z_Q^2 \hat{g}_s^{-1} \quad (2.13)$$

$$Z_N^{-1} = \left(-\frac{\partial \Pi_N(p)}{\partial \not{p}} \right)_{\not{p}=M_N} = Z_Q g_s \left(-\frac{\partial \hat{\Pi}_N(p)}{\partial \not{p}} \right)_{\not{p}=M_N} \equiv Z_Q g_s \hat{Z}_N^{-1}, \quad (2.14)$$

where $\hat{\Pi}_s$ and $\hat{\Pi}_N$ are defined in terms of the pole parts only:

$$\hat{\Pi}_s(q) = 6i \int \frac{d^4 k}{(2\pi)^4} \text{tr}_D [\gamma_5 S_F(k) \gamma_5 S_F(-(q-k))] \quad (2.15)$$

$$\hat{\Pi}_N(p) = i \int \frac{d^4 k}{(2\pi)^4} S_F(k) \Delta_{Fs}(p-k) \quad (2.16)$$

The equation of state of NM in the NJL model can be derived in a formal way [15] from the quark Lagrangian (2.2) by using hadronization techniques, but in the mean field approximation the resulting energy density of isospin symmetric NM has the simple form [11]

$$\mathcal{E} = \mathcal{E}_V - \frac{V_0^2}{4G_\omega} + 4 \int \frac{d^3 p}{(2\pi)^3} \Theta(p_F - |\mathbf{p}|) \epsilon_p, \quad (2.17)$$

where the vacuum contribution (quark loop) is

$$\mathcal{E}_V = 12i \int \frac{d^4 k}{(2\pi)^4} \ln \frac{k^2 - M^2 + i\epsilon}{k^2 - M_0^2 + i\epsilon} + \frac{(M-m)^2}{4G_\pi} - \frac{(M_0-m)^2}{4G_\pi}. \quad (2.18)$$

³We also note that such a renormalization procedure is no longer possible when one considers the pion cloud effects around the *nucleon*, which goes beyond the simple ladder approximation on the quark level.

Here M_0 the constituent quark mass for zero nucleon density. The condition $\partial\mathcal{E}/\partial V_0 = 0$ leads to $V_0 = 6 G_\omega \rho$, and we can eliminate the vector field in (2.17) in favor of the baryon density. The resulting expression has then to be minimized with respect to the constituent quark mass M for fixed density. For zero density this condition becomes identical to the familiar gap equation of the NJL model[10], and for finite density the nonlinear M -dependence of the nucleon mass M_N is essential to obtain saturation of the binding energy per nucleon [11].

In order to fully define the model one has to specify a cut-off procedure. In the calculations in this paper we will use the proper time regularization scheme [22, 11], where one evaluates loop integrals over a product of propagators by introducing Feynman parameters, performing a Wick rotation and replacing the denominator (A) of the loop integral according to

$$\frac{1}{A^n} \rightarrow \frac{1}{(n-1)!} \int_{1/\Lambda_{\text{UV}}^2}^{1/\Lambda_{\text{IR}}^2} d\tau \tau^{n-1} e^{-\tau A} \quad (n \geq 1), \quad (2.19)$$

where Λ_{IR} and Λ_{UV} are the infrared and ultraviolet cut-offs, respectively. The infrared cut-off plays the important role of eliminating the unphysical thresholds for the decay of the nucleon and mesons into quarks [22], thereby taking into consideration a particular aspect of confinement physics.

3 Nucleon electromagnetic form factors

The electromagnetic current of the nucleon in the quark-diquark model is represented by the Feynman diagrams of Fig.1 and given by

$$j_N^\mu(q) = \bar{\Gamma}_N(p') \int \frac{d^4k}{(2\pi)^4} \left[(S(p' - k) \Lambda_Q^\mu S(p - k)) \tau_s(k) + i (\tau_s(p' - k) \Lambda_D^\mu \tau_s(p - k)) S(k) \right] \Gamma_N(p). \quad (3.1)$$

Here Λ_Q^μ and Λ_D^μ are the electromagnetic vertices of the quark and the scalar diquark, both depending on the final and initial particle momenta. It

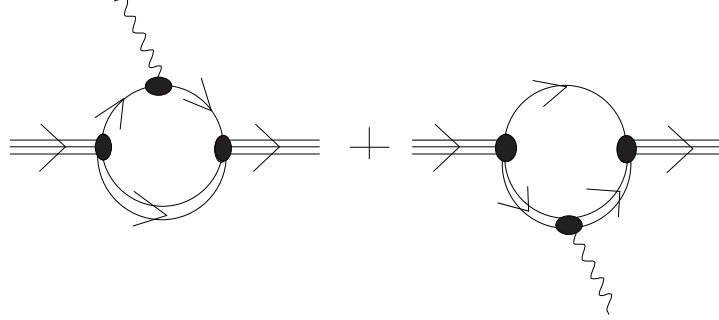


Figure 1: Feynman graphs for the evaluation of the nucleon electromagnetic current in the quark-diquark model. The double line represents the diquark t-matrix, the solid line the constituent quark propagator, and the black areas are the vertex functions and electromagnetic vertices.

is an easy task to use the Ward-Takahashi identities [23] for the quark and diquark vertices

$$q_\mu (S(\ell') \Lambda_Q^\mu S(\ell)) = -Q_Q (S(\ell') - S(\ell)) \quad (3.2)$$

$$q_\mu (\tau_s(\ell') \Lambda_D^\mu \tau_s(\ell)) = iQ_D (\tau_s(\ell') - \tau_s(\ell)) \quad (3.3)$$

to show the current and charge conservation for the nucleon:

$$q_\mu j_N^\mu(q) = Q_N \bar{\Gamma}_N(p') (\Pi_N(p') - \Pi_N(p)) \Gamma_N(p) = 0 \quad (3.4)$$

$$j^\mu(0) = Q_N \frac{p^\mu}{E_{Np}}, \quad (3.5)$$

where the electric charge of the nucleon $Q_N = Q_Q + Q_D$ is the sum of the quark and diquark electric charges.

The electromagnetic vertices in (3.1) describe the finite extension of the constituent quarks and the diquark. In general, they should be calculated off-shell consistently with the propagators τ_s and S , using Feynman diagrams or some ansatz which satisfies the Ward identities[8]. In the present work, however, our principal aim is to investigate the medium effects in a simple model calculation. For this purpose, we limit the complications caused by

the quark and diquark sizes to a minimum, and use an on-shell (or pole) approximation for the quark and diquark currents appearing in Eq.(3.1):

$$\left(S(\ell') \Lambda_Q^\mu S(\ell) \right) \longrightarrow Z_Q \left(S_F(\ell') \hat{\Lambda}_Q^\mu S_F(\ell) \right) \quad (3.6)$$

$$\left(\tau_s(\ell') \Lambda_D^\mu \tau_s(\ell) \right) \longrightarrow -g_s \left(\Delta_{Fs}(\ell') \hat{\Lambda}_D^\mu \Delta_{Fs}(\ell) \right), \quad (3.7)$$

where the on-shell (o.s.) vertices are denoted by a hat and given by the pole residues of the full quantities by

$$\hat{\Lambda}_Q^\mu \equiv Z_Q \left(\Lambda_Q^\mu \right)_{\text{o.s.}} \equiv \gamma^\mu F_{1Q}(q^2) + \frac{i\sigma^{\mu\nu} q_\nu}{2M} F_{2Q}(q^2) \quad (3.8)$$

$$\hat{\Lambda}_D^\mu \equiv g_s \left(\Lambda_D^\mu \right)_{\text{o.s.}} \equiv (\ell' + \ell)^\mu F_D(q^2). \quad (3.9)$$

Here we introduced the quark and diquark form factors which satisfy $F_{1Q}(0) = Q_Q$, $F_D(0) = Q_D$.

To understand (3.6) and (3.7), we note that in general the on-shell approximation for a vertex function $\Lambda^\mu(\ell', \ell)$ can be formulated only if it appears between pole parts of Green functions, because only in this case one can approximate it by its value for on-shell momenta ℓ', ℓ ⁴. This is why in Eq.(3.6) and (3.7) we have replaced the propagators left and right to the vertex functions by their pole parts (see (2.11) and (2.12)), which is also essential in order to have charge conservation with the vertices (3.8) and (3.9).

We now can write down the form of the nucleon current (3.1) which will be used in the further calculations:

$$j_N^\mu(q) = \sqrt{\frac{M_N}{E_{Np}} \frac{M_N}{E_{Np'}}} \bar{u}_N(p') \left(\mathcal{O}_C^\mu + \mathcal{O}_Q^\mu + \mathcal{O}_D^\mu \right) u_N(p). \quad (3.10)$$

Here the first and second terms denote the contributions of the contact term and the pole term of the diquark t-matrix to the quark diagram (first diagram

⁴This approximation is the basis of the standard convolution formalism to calculate quark light-cone momentum distributions and structure functions.

of Fig.1), and the third term is the contribution from the diquark diagram:

$$\mathcal{O}_C^\mu = -\frac{4iG_s}{\hat{g}_s}\hat{Z}_N \int \frac{d^4k}{(2\pi)^4} S_F(p' - k) \left(\gamma^\mu F_{1Q}(q^2) + \frac{i\sigma^{\mu\nu}q_\nu}{2M} F_{2Q}(q^2) \right) S_F(p - k) \quad (3.11)$$

$$\mathcal{O}_Q^\mu = i\hat{Z}_N \int \frac{d^4k}{(2\pi)^4} S_F(p' - k) \left(\gamma^\mu F_{1Q}(q^2) + \frac{i\sigma^{\mu\nu}q_\nu}{2M} F_{2Q}(q^2) \right) S_F(p - k) \Delta_{Fs}(k) \quad (3.12)$$

$$\mathcal{O}_D^\mu = i\hat{Z}_N F_D(q^2) \int \frac{d^4k}{(2\pi)^4} \Delta_{Fs}(p' - k) (p + p' - 2k)^\mu \Delta_{Fs}(p - k) S_F(k). \quad (3.13)$$

(For the contact term, we replaced $G_s \rightarrow G_s/Z_Q^2$, so that G_s in (3.11) is the renormalized coupling in the sense explained in Sect.2.) By using the elementary Ward-Takahashi identities $\not{q} = S_F^{-1}(\ell') - S_F^{-1}(\ell)$ and $\ell'^2 - \ell^2 = \Delta_{Fs}^{-1}(\ell') - \Delta_{Fs}^{-1}(\ell)$ and the fact that on the nucleon mass shell $\Pi_N(p) = \Pi_N(p')$, it is easy to check that the 3 parts in (3.10) satisfy current conservation separately⁵. Similarly, charge conservation can be checked by using the elementary Ward identities $\gamma^\mu = \partial S_F^{-1}(\ell)/\partial \ell^\mu$ and $2\ell^\mu = \partial \Delta_{Fs}^{-1}(\ell)/\partial \ell^\mu$, as well as $F_{1Q}(0) = Q_Q$, $F_D(0) = Q_D$. It has to be noted, however, the general Ward-Takahashi identity for an *off-shell* nucleon (the first equality in Eq.(3.4) without the nucleon spinor) is not valid in this approximation scheme.

It is not very difficult to evaluate the three loop integrals in (3.11)-(3.13), and in Appendix A the results are given in terms of the Dirac-Pauli form factors F_{1N} and F_{2N} , which are defined by

$$j_N^\mu = \sqrt{\frac{M_N}{E_{Np}} \frac{M_N}{E_{Np'}}} \bar{u}_N(p') \left[\gamma^\mu F_{1N}(q^2) + \frac{i\sigma^{\mu\nu}q_\nu}{2M_N} F_{2N}(q^2) \right] u_N(p). \quad (3.14)$$

In the following we will discuss various steps in the calculation of the nucleon form factors.

⁵These formal manipulations involve shifts of the integration variables. In the actual calculations based on our regularization scheme, however, we always checked that current and charge conservation are satisfied exactly. (Therefore, the explicit expressions given in the Appendices all satisfy the charge conservation.)

3.1 Naive quark-diquark model

The simplest approximation consists in assuming point couplings of the quarks and diquarks to the photon, i.e., replacing $F_{1Q} \rightarrow Q_Q = \frac{1}{6} + \frac{\tau_3}{2}$, $F_{2Q} \rightarrow 0$, $F_D \rightarrow Q_D = \frac{1}{3}$ in Eqs. (3.11)-(3.13). This approximation will be called the “naive quark-diquark model”, and the detailed expressions can be found in Appendix A.

3.2 Effects of finite diquark size

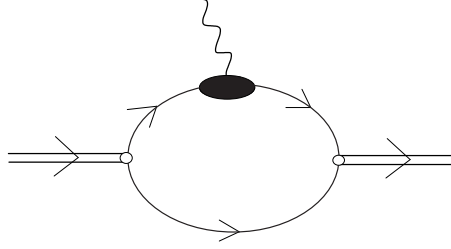


Figure 2: Graphical representation of the diquark form factor. The white circles denote the diquark vertex functions, and the black area is the quark electromagnetic vertex. (There is a second diagram where the photon couples to the other quark, but also an overall symmetry factor $\frac{1}{2}$.)

Here we consider the effect of the diquark form factor F_D , which has been defined in (3.9). The vertex Λ_D^μ is shown graphically in Fig.2, where the quark-diquark vertex functions are those appearing in the Lagrangian(2.3). We obtain

$$\hat{\Lambda}_D^\mu = i g_s \int \frac{d^4 k}{(2\pi)^4} \left\{ \text{Tr} \left[\gamma_5 S(p' + k) \Lambda_Q^\mu S(p + k) \gamma_5 S(k) \right] \right\}, \quad (3.15)$$

where the trace refers to color, isospin and Dirac indices. Using the on-shell approximation (3.6), the definition of quark form factors (3.8), and also

(2.12) and (2.13), we obtain

$$\begin{aligned}\hat{\Lambda}_D^\mu &= 6i\hat{g}_s \int \frac{d^4k}{(2\pi)^4} \left\{ F_{1Q}^{(0)}(Q^2) \text{Tr}_D [\gamma_5 S_F(p' + k) \gamma^\mu S_F(p + k) \gamma_5 S_F(k)] \right. \\ &\quad \left. + F_{2Q}^{(0)}(Q^2) \text{Tr}_D \left[\gamma_5 S_F(p' + k) \frac{i\sigma^{\mu\nu} q_\nu}{2M} S_F(p + k) \gamma_5 S_F(k) \right] \right\}. \quad (3.16)\end{aligned}$$

Here $F_{1Q}^{(0)}$ and $F_{2Q}^{(0)}$ are the isoscalar parts of the quark form factors F_{1Q} and F_{2Q} . The resulting diquark form factor F_D is given in Appendix A.

3.3 Effects of meson cloud around constituent quarks

Here we consider the quark form factors arising from the pion cloud and vector mesons. For the pion cloud, we obtain from the definition (3.8) and the Feynman diagrams of Fig.3,

$$\begin{aligned}\hat{\Lambda}_Q^\mu &= Z_Q \gamma^\mu Q_Q + Z_Q \int \frac{d^4k}{(2\pi)^4} \left[-\gamma_5 \tau_i (S(p' - k) \Lambda_{Q0}^\mu S(p - k)) \tau_i \gamma_5 \tau_\pi(k) \right. \\ &\quad \left. + i (\tau_\pi(p' - k) \Lambda_\pi^\mu \tau_\pi(p - k)) \gamma_5 S(k) \gamma_5 \right]. \quad (3.17)\end{aligned}$$

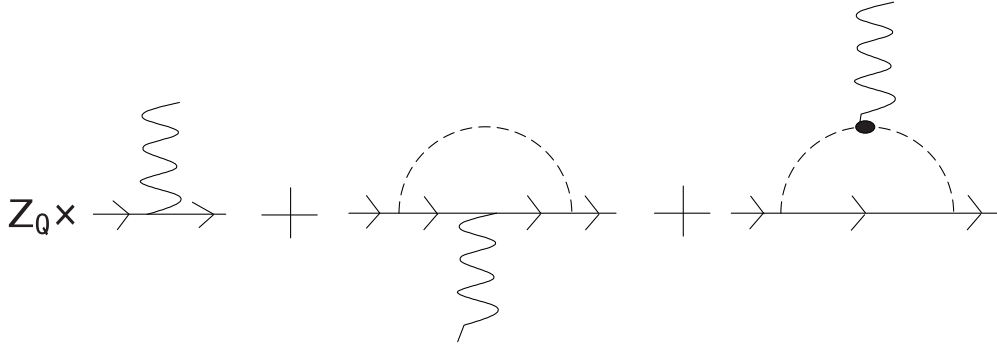


Figure 3: Pion cloud contributions to the quark electromagnetic vertex. Z_Q is the quark wave function renormalization factor, and the dashed line represents the t-matrix in the pion channel. (This figure actually refers to the expression (3.25), where the factor Z_Q remains only for the “bare” term.)

Here τ_π is the reduced $q\bar{q}$ t-matrix in the pion channel, which can be

approximated in the same way as the diquark t-matrix (2.11):

$$\tau_\pi(k) = \frac{-2iG_\pi}{1 + 2G_\pi\Pi_\pi(k^2)} \longrightarrow -2iG_\pi + \frac{ig_\pi}{k^2 - M_\pi^2} \equiv -2iG_\pi + ig_\pi\Delta_{F\pi}(k). \quad (3.18)$$

The bubble graph in the pion channel is $\Pi_\pi = \Pi_s$ (see (2.5)), and the residue g_π will be given in Eq.(3.24) below.

The expression (3.17) is formally similar to the nucleon current (3.1). The presence of the first term simply expresses the fact that in the NJL model the (bare) quarks are present from the beginning, and the factor Z_Q gives the probability of having a constituent quark without its pion cloud. It has been expressed in Eq.(2.12) in terms of the self energy

$$\Sigma_Q(p) = -3 \int \frac{d^4k}{(2\pi)^4} (\gamma_5 S(p-k) \gamma_5) \tau_\pi(k). \quad (3.19)$$

The quark electromagnetic vertex Λ_{Q0}^μ in (3.17) will be approximated by its point form after processing the renormalization factor Z_Q , and the pion electromagnetic vertex $\Lambda_\pi^\mu \equiv \tau_i \Lambda_{\pi,ij}^\mu \tau_j$ is similar to the diquark vertex of Fig.2, but with point quark-photon couplings, as will be specified below.

We now follow the same steps as for the calculation of the nucleon current: We use the on-shell approximation for the quark and pion vertices

$$(S(\ell') \Lambda_{Q0}^\mu S(\ell)) \longrightarrow Z_Q (S_F(\ell') \hat{\Lambda}_{Q0}^\mu S_F(\ell)) \quad (3.20)$$

$$(\tau_\pi(\ell') \Lambda_\pi^\mu \tau_\pi(\ell)) \longrightarrow -g_\pi (\Delta_{F\pi}(\ell') \hat{\Lambda}_\pi^\mu \Delta_{F\pi}(\ell)), \quad (3.21)$$

where the on-shell vertices are defined by

$$\hat{\Lambda}_{Q0}^\mu \equiv Z_Q (\Lambda_{Q0}^\mu)_{\text{o.s.}} \equiv \gamma^\mu Q_Q \quad (3.22)$$

$$\hat{\Lambda}_{\pi,ij}^\mu \equiv g_\pi (\Lambda_{\pi,ij}^\mu)_{\text{o.s.}} \equiv (\ell' + \ell)^\mu (-i\epsilon_{ij3}) F_\pi(q^2). \quad (3.23)$$

Using $S(k) = Z_Q S_F(k)$ in the expression for Π_π , we get

$$g_\pi^{-1} = \left(-\frac{\partial \Pi_\pi(q)}{\partial q^2} \right)_{q^2=M_\pi^2} = Z_Q^2 \left(-\frac{\partial \hat{\Pi}_\pi(q)}{\partial q^2} \right)_{q^2=M_\pi^2} \equiv Z_Q^2 \hat{g}_\pi^{-1}, \quad (3.24)$$

with the renormalized bubble graph $\hat{\Pi}_\pi = \hat{\Pi}_s$, see (2.15). Then Eq. (3.17) becomes

$$\begin{aligned}\hat{\Lambda}_Q^\mu &= Z_Q \gamma^\mu Q_Q - i \hat{g}_\pi \frac{1}{2} (1 - \tau_3) \int \frac{d^4 k}{(2\pi)^4} \gamma_5 (S_F(p' - k) \gamma^\mu S_F(p - k)) \gamma_5 \Delta_{F\pi}(k) \\ &- 2i \tau_3 \hat{g}_\pi F_\pi(q^2) \int \frac{d^4 k}{(2\pi)^4} (\Delta_{F\pi}(p' - k) (p' + p - 2k)^\mu \Delta_{F\pi}(p - k)) \gamma_5 S_F(k) \gamma_5.\end{aligned}\quad (3.25)$$

Here we note that the contribution of the contact term ($2iG_\pi$) to the quark diagram has been dropped in order to avoid double counting: Because we always assume that our interaction Lagrangians are Fierz symmetric, it is easy to see that this contribution can be incorporated into the vector meson channel, which will be separately considered below. By using $S = Z_Q S_F$ in the self energy (3.19) and in the expression for Z_Q of Eq.(2.12), we see that

$$Z_Q = 1 + \left(\frac{\partial \hat{\Sigma}_Q}{\partial \not{p}} \right)_{\not{p}=M}, \quad (3.26)$$

where the renormalized quark self energy is given by

$$\hat{\Sigma}_Q(p) = -3i \hat{g}_\pi \int \frac{d^4 k}{(2\pi)^4} (\gamma_5 S_F(p - k) \gamma_5) \Delta_{F\pi}(k). \quad (3.27)$$

The further evaluation of the loop integral (3.25) is left to Appendix B, where the contributions to the quark form factors F_{1Q} and F_{2Q} are given. The pion electromagnetic vertex is evaluated from the definition (3.23) and a Feynman diagram similar to Fig.2 for an external pion, but with a point quark-photon coupling:

$$\hat{\Lambda}_{ij}^\mu = (-i \epsilon_{ij3}) 6i \hat{g}_\pi \int \frac{d^4 k}{(2\pi)^4} \text{Tr}_D [\gamma_5 S_F(p' + k) \gamma^\mu S_F(p + k) \gamma_5 S_F(k)]. \quad (3.28)$$

The explicit form of $F_\pi(q^2)$ is given in Appendix B.

Finally, we consider the corrections of the quark electromagnetic vertex arising from vector mesons, similar to vector meson dominance (VMD) models. If our original interaction Lagrangian contains terms of the form

$$\mathcal{L}_{I,v} = -G_\omega (\bar{\psi} \gamma^\mu \psi)^2 - G_\rho (\bar{\psi} \gamma^\mu \boldsymbol{\tau} \psi)^2, \quad (3.29)$$

then the point-like quark-photon vertices in the diagrams of Fig.3 and the pion vertex Λ_π^μ are replaced by the VMD vertex shown in Fig.4.

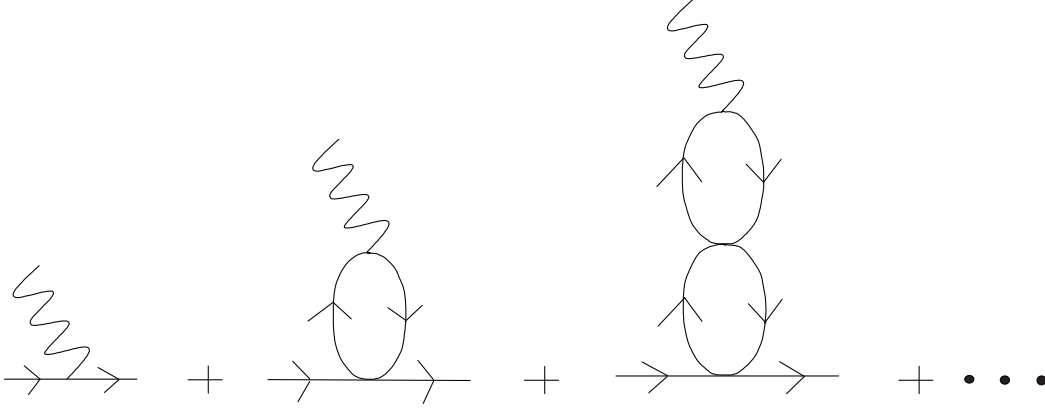


Figure 4: The corrections to the quark electromagnetic vertex arising from vector meson dominance. Here the 4-fermi interactions refer to the vector channel (see Eq.(3.29)), i.e., terms with tensor coupling to the external quark are not included.

Because of the transverse structure of the bubble graphs in the vector channel, this leads to the following renormalization:

$$\gamma^\mu Q_Q \longrightarrow \frac{1}{6} \left[\gamma^\mu - \frac{2G_\omega \hat{\Pi}_V(q^2)}{1 + 2G_\omega \hat{\Pi}_V(q^2)} \left(\gamma^\mu - \frac{q^\mu \not{q}}{q^2} \right) \right] \quad (3.30)$$

$$+ \frac{\tau_3}{2} \left[\gamma^\mu - \frac{2G_\rho \hat{\Pi}_V(q^2)}{1 + 2G_\rho \hat{\Pi}_V(q^2)} \left(\gamma^\mu - \frac{q^\mu \not{q}}{q^2} \right) \right], \quad (3.31)$$

where the form of $\hat{\Pi}_V$ is given in Appendix B. Because our quark-photon vertex in (3.8) is defined for on-shell quarks, the terms $\propto \frac{q^\mu \not{q}}{q^2}$ do not contribute.

Therefore the isoscalar (or isovector) parts in the quark electromagnetic vertex should be multiplied by a form factor ⁶ $F_\omega(q^2)$ (or $F_\rho(q^2)$), where

$$F_\alpha(q^2) = \frac{1}{1 + 2G_\alpha \hat{\Pi}_V(q^2)} \quad (\alpha = \omega, \rho). \quad (3.32)$$

4 Results for the nucleon form factors

In this section we will show our results for the nucleon form factors. First we discuss our model parameters and particle masses. The parameters are the same as in Refs.[11, 15]: The IR cut-off Λ_{IR} is fixed as 0.2 GeV, the constituent quark mass at zero nucleon density is $M_0 = 0.4$ GeV, and G_π , Λ_{UV} are determined so as to reproduce $M_\pi = 0.14$ GeV and $f_\pi = 93$ MeV. This gives $G_\pi = 19.60 \text{ GeV}^{-2}$ and $\Lambda_{\text{UV}} = 0.6385$ GeV. The coupling constant G_s is determined so as to reproduce $M_{N0} = 0.94$ GeV, which gives the ratio $G_s/G_\pi = 0.508$. The coupling constant G_ω is determined so that the curve for the NM binding energy per nucleon (E_B/A) as a function of the density passes through the empirical saturation point⁷ $(\rho, E_B/A) = (0.16 \text{ fm}^{-3}, 15 \text{ MeV})$, which gives the ratio $G_\omega/G_\pi = 0.37$. Finally, for the VMD form factors (3.32) we also need the coupling constant G_ρ , which is determined by reproducing the empirical symmetry energy coefficient $a_4 = 35$ MeV at the density $\rho = 0.16 \text{ fm}^{-3}$, which gives $G_\rho/G_\pi = 0.091$.

In Table 1 we list the effective quark, diquark, nucleon and pion masses for the densities $\rho = 0, 0.08, 0.16$, and 0.24 fm^{-3} . Concerning the pion mass in the medium, we use a general result based on chiral symmetry [25], which for the NJL model implies that the product $M_\pi^2 \cdot M$ is a constant independent

⁶Because the scalar diquark has isospin zero, this eventually also holds for the nucleon electromagnetic vertex.

⁷We recall from Ref.[11] that, in this simple NJL model, we cannot adjust both the empirical binding energy and saturation density at the same time. Therefore, although the binding energy curve passes through the empirical saturation point, its minimum is at a different point, $(\rho, E_B/A) = (0.22 \text{ fm}^{-3}, 17.3 \text{ MeV})$.

of density, see Eq.(2.58) of Ref.[11]. We therefore use ⁸ $M_\pi^2 = M_{\pi 0}^2 \cdot M_0/M$. Also listed in Table 1 are the values of \hat{g}_s , \hat{g}_π , \hat{Z}_N and Z_Q .

	$\rho = 0$	$\rho = 0.08 \text{ fm}^{-3}$	$\rho = 0.16 \text{ fm}^{-3}$	$\rho = 0.24 \text{ fm}^{-3}$
M	0.4	0.353	0.308	0.268
M_s	0.576	0.493	0.413	0.342
M_N	0.94	0.818	0.707	0.619
M_π	0.14	0.149	0.159	0.171
\hat{g}_s	18.26	17.17	16.20	15.40
\hat{g}_π	17.81	14.29	11.60	9.70
\hat{Z}_N	44.32	47.62	50.38	51.97
Z_Q	0.808	0.832	0.852	0.869

Table 1: Effective masses for the quark, the diquark, the nucleon and the pion (all in GeV), and pole residues \hat{g}_s , \hat{g}_π , \hat{Z}_N and Z_Q for four values of the density.

We will discuss our results for the nucleon form factor in terms of the Dirac-Pauli form factors defined by Eq.(3.14). In the discussion of medium effects, in particular the effects of the reduced nucleon mass ($M_N < M_{N0}$), we will also refer to an equivalent parametrization in terms of the “orbital form factor” G_L and the “spin form factor” G_S :

$$j_N^\mu = \sqrt{\frac{M_N}{E_{Np}} \frac{M_N}{E_{Np'}}} \bar{u}_N(p') \left[\frac{(p' + p)^\mu}{2M_{N0}} G_L(q^2) + \frac{i\sigma^{\mu\nu} q_\nu}{2M_{N0}} G_S(q^2) \right] u_N(p) \quad (4.1)$$

The relations to the Dirac-Pauli form factors are

$$G_L = \frac{M_{N0}}{M_N} F_{1N}, \quad G_S = \frac{M_{N0}}{M_N} (F_{1N} + F_{2N}). \quad (4.2)$$

⁸More precisely, this pion mass is defined at zero momentum, and includes nucleonic (Z-graph and contact) terms, which are important in order to guarantee the Goldstone nature of the pion in the medium. We note that these nucleonic contributions to the scalar diquark (or sigma) mass at normal densities are numerically small compared to the qq (or $q\bar{q}$) polarizations, although they become important for small M and guarantee the stability of the system w.r.t. variations in M , see Ref.([11]) for details.

We introduce these form factors here, because F_1 and F_2 do not directly reflect the enhancement of the nucleon orbital current ($\mathbf{j}_{N,\text{orb}}$) arising from the reduced nucleon mass (enhanced nuclear magneton)⁹. Moreover, the parametrization (4.1) for the space part of the current has more connection to the traditional calculations of nuclear magnetic properties [28], because the values of these form factors at $q = 0$ reduce to the orbital and spin g-factors: $g_L = G_L(0)$, $g_S = G_S(0)$.

Here we would like to point out that these different ways to discuss the medium modifications of the nucleon current remind us that the form factors of a nucleon in the medium are not directly observable quantities: Ultimately the current j_N^μ has to be used in a nuclear structure calculation of observable cross sections. Our current j_N^μ reflects only those effects which are not taken into account in nuclear structure calculations, i.e., the effects of the nuclear mean fields on the internal motion of quarks in the nucleon. Other effects, which explicitly depend on the density and have their origin in the Pauli principle on the level of nucleons, must be considered in the nuclear part of the calculation¹⁰. As an example of such a calculation for the case of nuclear matter, we will consider the response function for quasielastic electron scattering in Sect.5.

For the zero density (single nucleon) case, it is possible to define a Breit frame where $q_0 = 0$, and in this frame the nucleon current can be expressed in terms of the familiar electric and magnetic form factors

$$G_E(q^2) = F_1(q^2) + \frac{q^2}{4M_N^2} F_2(q^2) \quad (4.3)$$

$$G_M(q^2) = F_1(q^2) + F_2(q^2). \quad (4.4)$$

⁹Note that the appearance of the medium modified nucleon mass (M_N) in the Pauli term of (3.14) is a mere definition of F_2 .

¹⁰This is also evident from the fact that the full current of a nucleon in the medium, including the explicitly density dependent parts, cannot be parametrized in the Lorentz invariant forms (3.14) or (4.1).

We will compare our calculated form factors for zero density with the empirical dipole form factors, defined by

$$\begin{aligned} G_{Ep} &= G_{Mp}/\mu_p = G_{Mn}/\mu_n = \frac{1}{(1 - q^2/0.71 \text{ GeV}^2)^2} \\ F_{1n} &= 0. \end{aligned} \quad (4.5)$$

For a nucleon moving in the medium, however, one cannot define a Breit frame, and consequently the combinations (4.3) and (4.4) do not enter naturally in the expressions for nuclear observables, like response functions or elastic form factors. For the finite density case we will therefore discuss our results in terms of the form factors F_1 and F_2 , or G_L and G_S .

The results for the form factors at zero density (free nucleon case) are shown in Figs.5-8. There we plot (i) the results of the naive quark-diquark model (see Sect.3.1) without (dotted lines) and with (dashed lines) the contact term contribution to the quark diagram of Fig.1, (ii) the results obtained by including in addition the effects of the diquark form factor (dash-dotted lines), and (iii) the total result including also the pion and VMD effects.

Fig. 5 shows that in the naive quark-diquark model the electric size of the proton is too small and the form factors F_{1p} and G_{Ep} fall off too slowly. The situation improves when the diquark form factor is included, and also the pion cloud gives some positive contribution to the electric size of the proton¹¹. The total result for F_{1p} still lies above the empirical dipole form factor, but we can expect that the further inclusion of axial vector diquarks and pion cloud effects around the *nucleon* will lead to a satisfactory description.

Fig. 6 shows that the proton magnetic moment in the naive quark-diquark picture is too small, which is expected and also well known[17, 24]. The finite

¹¹We obtain $\langle r_E^2 \rangle_p = 0.421 \text{ fm}^2 + 0.062 \text{ fm}^2 = 0.483 \text{ fm}^2$, where the two terms come from the Dirac (F_1) part and the anomalous (F_2) part. The fact that this is too small compared to the experimental value of 0.74 fm^2 is partially because the magnetic moment is too small, but also because the slope of F_1 is too small.

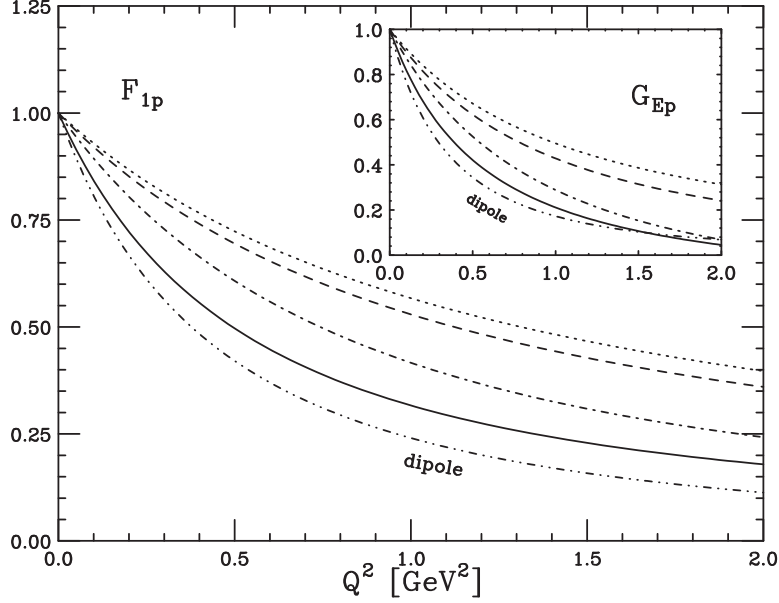


Figure 5: The form factor F_{1p} for zero density. The dotted line is the result of the naive quark-diquark model without the contact term, to which the other contributions are successively added as follows: Dashed line: including contact term; dash-dotted line: including diquark form factor; solid line: full results including pion and vector meson contributions. The dash-double dotted line labeled “dipole” shows the dipole parametrization. The insert shows the form factor G_{Ep} , with the same meaning of the lines.

size effects of the scalar diquark do not contribute much in this case. The inclusion of the contact term in the quark diagram of Fig.1 improves the situation somewhat. By using a Fierz transformation, this term is actually seen to be equivalent to a vector meson contribution (like shown in Fig.4 for the quark), but with a tensor coupling ($\propto \sigma^{\mu\nu} q_\nu$) to the nucleon. Also the pion cloud, which leads to anomalous magnetic moments of the constituent up and down quarks¹², gives a positive contribution to the proton magnetic moment, but the total result is still too small. It is, however, known that the

¹²We obtain $\mu_u = \frac{2}{3} + 0.061$, $\mu_d = -\frac{1}{3} - 0.123$ for the magnetic moments of u,d quarks in the free nucleon.

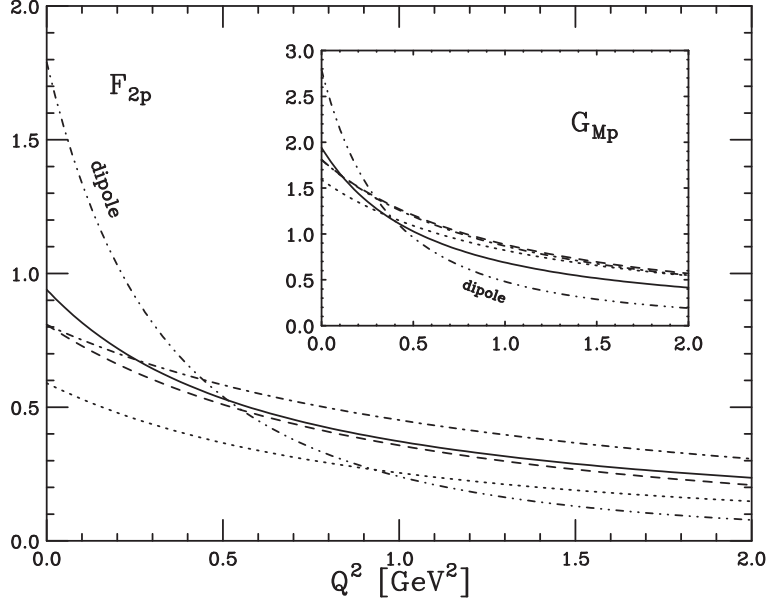


Figure 6: Same as Fig. 5 for the form factors F_{2p} (main part) and G_{Mp} (insert) for zero density.

axial vector diquark and the pion cloud around the *nucleon* give large contributions to the magnetic moment and the associated form factors, and Fig.6 shows how far one can go in the simple quark - scalar diquark description.

The importance of the diquark form factor is also seen for the neutron form factors F_{1n} and G_{En} , which are shown in Fig. 7. The naive quark-diquark model gives an electric form factor which is too large in comparison to the experimental one (note that the experimental G_{En} is smaller than the “dipole form factor” shown in Fig. 7), and the diquark form factor, which suppresses the (positive) contribution from the second diagram of Fig.1 relative to the (negative) first one, is essential to obtain reasonable values. The electric size of the neutron is somewhat too small in magnitude, but this is because the absolute value of the magnetic moment is too small ¹³.

¹³We obtain $\langle r_E^2 \rangle_n = 0.003 \text{ fm}^2 - 0.072 \text{ fm}^2 = -0.069 \text{ fm}^2$, where the two terms come

In this connection, it is interesting to observe that the result for F_{1n} , and in particular its contribution to the electric radius, is very small, and therefore the electric size of the neutron is almost entirely due to the “Foldy term” [26].

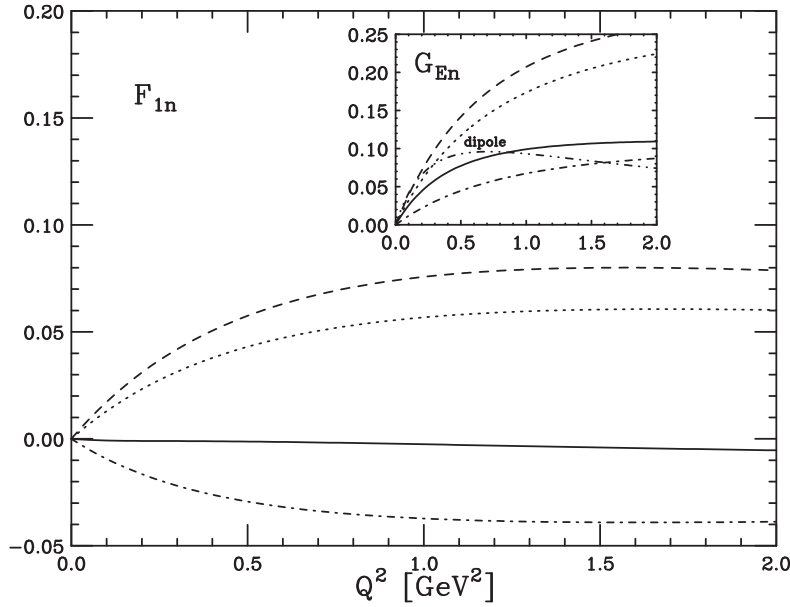


Figure 7: Same as Fig. 5 for the form factors F_{1n} (main part) and G_{En} (insert) for zero density. The dipole parametrization of F_{1n} is zero by definition and therefore not indicated here.

The situation for the form factors F_{2n} and G_{Mn} shown in Fig. 8 is similar to the case of the proton (Fig. 6), i.e., the contact term and the pion cloud around the constituent quarks give some improvements of the magnetic moment, but the total result is still too small. This, and the fact that the form factors fall off too slowly, again points out the necessity to include the axial from the Dirac (F_1) part and the anomalous (F_2) part. The fact that this is too small in magnitude compared to the experimental value of -0.12 fm^2 is because the absolute value of the magnetic moment is too small. For discussions on the role of these two contributions to the neutron electric radius, see for example [26].

vector diquark channel.

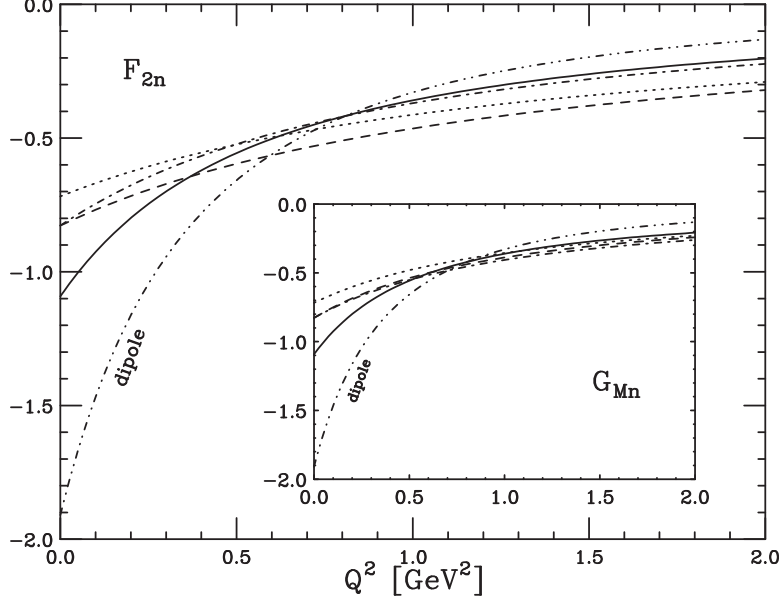


Figure 8: Same as Fig. 5 for the form factors F_{2n} (main part) and G_{Mn} (insert) for zero density.

The medium modifications of the nucleon form factors are shown in Figs. 9-12, where we plot the results for $\rho = 0$ (dotted lines), $\rho = 0.08 \text{ fm}^{-3}$ (dashed lines), $\rho = 0.16 \text{ fm}^{-3}$ (solid lines), and $\rho = 0.24 \text{ fm}^{-3}$ (dash-dotted lines).

The result for F_{1p} of Fig. 9 indicates that the electric size of the proton in the medium is somewhat enhanced. The orbital form factor G_{Lp} shown in the insert of Fig.9 demonstrates the enhancement of the orbital current ($\mathbf{j}_{N,\text{orb}}$) due to the reduced effective nucleon mass, see Eq.(4.2). We have to remind, however, that the isoscalar part of this enhancement is in a sense spurious, because in an actual nuclear calculation it is canceled by the “backflow” effect[27], which in our language arises from Z-graphs, i.e., the Pauli blocking part of the $N\bar{N}$ excitation piece (see the detailed discussions in Ref.[28, 29] on the backflow in relativistic meson-nucleon theories). Namely, the proton

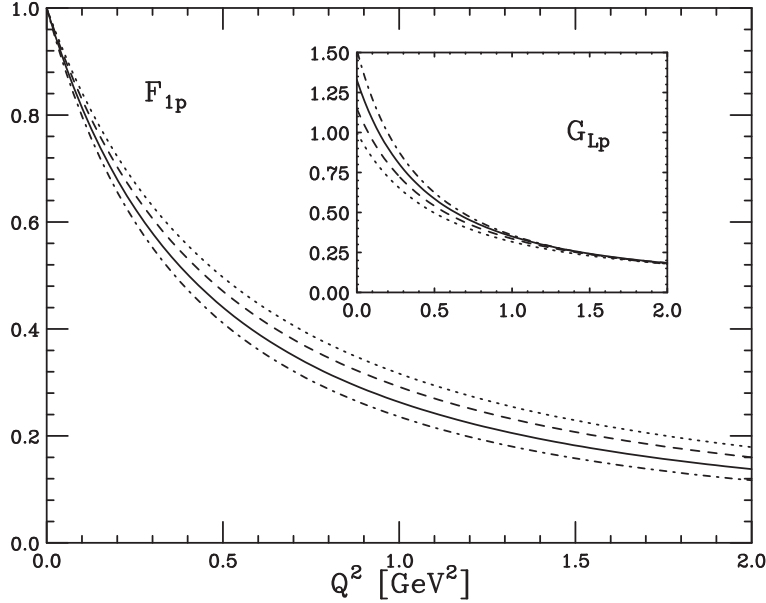


Figure 9: The form factor F_{1p} for the cases $\rho = 0$ (dotted line), $\rho = 0.08 \text{ fm}^{-3}$ (dashed line), $\rho = 0.16 \text{ fm}^{-3}$ (solid line), $\rho = 0.24 \text{ fm}^{-3}$ (dash-dotted line). The insert shows the proton orbital form factor G_{Lp} defined in Eq.(4.1) with the same meaning of the lines.

orbital g-factor, which is roughly M_{N0}/M_N in a Hartree calculation, becomes approximately $\frac{1}{2}(1 + M_{N0}/M_N)$ after the inclusion of the backflow, where the first term is the isoscalar and the second one the isovector piece¹⁴.

Fig. 10 shows that the medium effects tend to decrease the “intrinsic” anomalous magnetic moment of the proton, but when combined with the enhancement of the nuclear magneton, the spin g-factor is enhanced, as shown in the insert of Fig.10. It is interesting that a very similar result has been obtained also in hadronic models[18]. Therefore, the quark effects considered here do not lead to a quenching of the spin g-factor, as would be desirable to explain the missing quenching of isovector nuclear magnetic moments [28],

¹⁴It is well known that the pion effects further enhance the isovector piece[28].

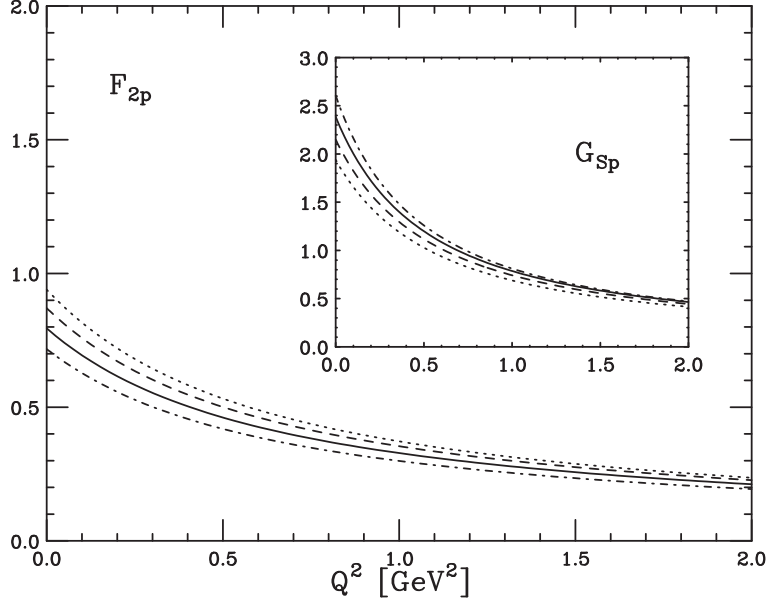


Figure 10: Same as Fig.9 for the form factor F_{2p} (main part) and the proton spin form factor G_{Sp} defined in Eq.(4.1) (insert).

but rather to an enhancement¹⁵. The figure also shows that the magnetic size of the proton becomes somewhat larger in the medium.

The results for the neutron form factor F_{1n} in Fig. 11 show that the effect of finite diquark size, which was very important for the zero density case (Fig.7) to reduce F_{1n} to reasonable values, increases with increasing density. That is, the diquark form factor at finite density further suppresses the positive contribution of the diquark diagram in Fig.1. The orbital form factor G_{Ln} shown in the insert of Fig.11 again demonstrates the enhancement of the nuclear magneton, but we have to keep in mind that the backflow effect will change the neutron orbital g-factor from the present value 0 to roughly $\frac{1}{2}(1 - M_{N0}/M_N) < 0$, and that effects of the pion cloud around the nucleon

¹⁵This is in contrast to the quenching of the axial vector coupling constant observed in the quark-diquark calculations of Ref.[14] including the axial vector diquark, and in hadronic models [30].

are known to further enhance the magnitude of the neutron orbital g-factor.

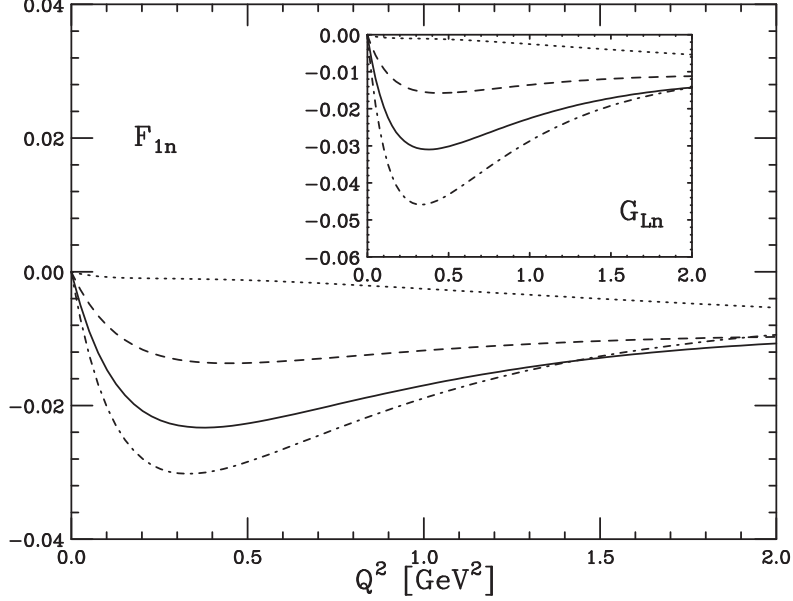


Figure 11: Same as Fig.9 for the form factor F_{1n} (main part) and the neutron orbital form factor G_{Ln} defined in Eq.(4.1) (insert).

The medium effects on the neutron form factor F_{2n} shown in Fig.12 are qualitatively similar to the proton case of Fig.10: They decrease the absolute value of the “intrinsic” anomalous magnetic moment of the neutron, but when combined with the enhancement of the nuclear magneton the neutron spin g-factor becomes slightly enhanced in magnitude, as shown in the insert of Fig.12. The magnetic size of the neutron is not changed much, and the total medium effects on the neutron spin form factor are very small.

An interesting common feature of the results shown in Fig. 9-12 is that the medium modifications of the orbital and spin form factors ($G_L(Q^2)$ and $G_S(Q^2)$) always decrease with increasing Q^2 . This is consistent with the intuitive expectation that the internal structure of the nucleon at short distances is not influenced much by the mean nuclear fields, and again indicates that

these form factors reflect the change of the nucleon current in the medium more directly and transparently than the form factors F_1 , F_2 themselves, or any other combination of them.

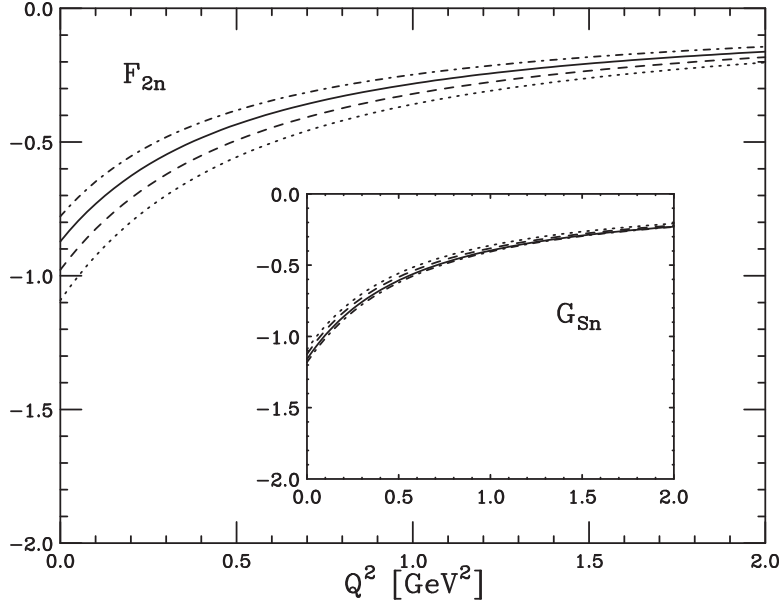


Figure 12: Same as Fig.9 for the form factor F_{2n} (main part) and the neutron spin form factor G_{Sn} defined in Eq.(4.1) (insert).

5 Application: The longitudinal nuclear response function

As an application of the medium effects discussed in the previous section to the calculation of nuclear quantities, we consider the longitudinal response function for quasielastic electron scattering. Generally, quasielastic processes are the ideal places to investigate medium modifications of nucleon form factors, because the on-shell kinematics, which is used in the derivation of the nucleon form factors, is justified. Recently, experiments on the polarization

transfer in proton knock-out reactions have been carried out in the region of quasielastic kinematics at large momentum transfers[5], and the results were discussed in connection to the predicted medium modifications of nucleon form factors[6]. In this work, however, we will consider the simpler case of the inclusive quasielastic response function in the region of lower momentum transfers. In previous works[31], based on purely hadronic models, it was shown that this quantity is quite sensitive to medium modifications of form factors, and here we wish to apply our more microscopic quark description to the longitudinal response function in nuclear matter.

The longitudinal response function in isospin symmetric nuclear matter is expressed as

$$S_L(\omega, \mathbf{q}) = \frac{2Z}{\pi\rho} \text{Im} \Pi_L(\omega, \mathbf{q}), \quad (5.1)$$

where $\Pi_L(\omega, \mathbf{q})$ is the 2-point (correlation) function for two external operators j_N^0 . In the mean field (Hartree) approximation, this is expressed by the first diagram of Fig.13, and if we include the direct terms of the NN interaction in the ladder approximation, this gives the familiar RPA series.

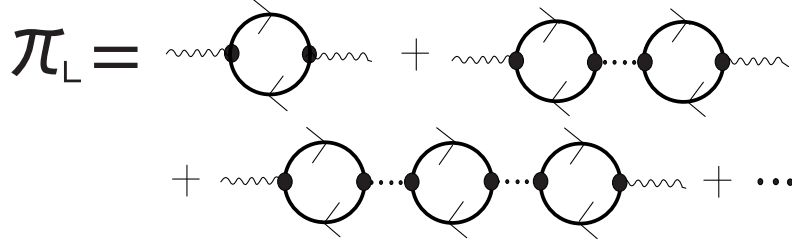


Figure 13: Graphical representation of the longitudinal current-current correlation function. The solid lines represent nucleons, and the dashed lines the interaction between nucleons. The external operator is j_N^0 . The first diagram gives the Hartree response function, and the others the RPA corrections.

The relativistic calculation of Π_L follows the lines given in Ref.[32, 33], i.e., the bubble graphs in Fig.13 consist of the nucleon particle- nucleon hole

excitations and the Pauli blocking part of the nucleon particle- antinucleon excitations (Z-graphs). The other effects, which are not taken into account explicitly in Fig.13, are summarized in the density dependent electromagnetic vertices. Previous calculations based on hadronic models[31] incorporated the vacuum fluctuations on the level of nucleons (that is, the change of the nucleon-antinucleon vacuum polarization graphs in the presence of the nuclear mean fields), but it is more appropriate to describe these vacuum fluctuations on the level of quarks ¹⁶. Therefore we use our nucleon current (3.1) for $\mu = 0$ at the electromagnetic vertices of Fig.13.

For the RPA calculation, we need the NN interaction kernel in our effective quark theory, which is shown graphically in Fig.14 and expressed as ¹⁷

$$V_{NN}(k) \equiv V_\sigma(k) (\mathbf{1})_1 \cdot (\mathbf{1})_2 + V_\omega(k) (\gamma_\mu)_1 \cdot (\gamma_\mu)_2 \quad (5.2)$$

$$= \frac{-2G_\pi}{1 - 2G_\pi \hat{\Pi}_\sigma(k^2) + 2G_\pi \delta M_s^2} \left(\frac{dM_N}{dM} \right)^2 F_\sigma^2(k^2) (\mathbf{1})_1 \cdot (\mathbf{1})_2 \quad (5.3)$$

$$+ \frac{2G_\omega}{1 + 2G_\omega \hat{\Pi}_V(k^2)} 9 F_\omega^2(k^2) (\gamma_\mu)_1 \cdot (\gamma_\mu)_2 \quad (5.4)$$

Here the first factor in (5.3) is the reduced $q\bar{q}$ t-matrix in the sigma meson channel, and the corresponding bubble graph $\hat{\Pi}_\sigma$ is given in Appendix C. The derivation of the effective NN interaction in the NJL model[11], however, has shown that in addition to the part $\hat{\Pi}_\sigma$, which describes the $q\bar{q}$ exchange (see Fig.14), there is also a nuclear part which consists of (i) the Z-graph, and (ii) a contact term arising from an induced $\bar{N}\sigma^2 N$ interaction. Concerning

¹⁶Although this follows naturally from the derivation of the nucleon lagrangian from the quark lagrangian in the path integral approach [15], or from the derivation of the effective NN interaction in quark theories following the Landau-Migdal approach[11], it remains to be demonstrated explicitly for electromagnetic quantities.

¹⁷The quantities $(\mathbf{1})_i$ and $(\gamma^\mu)_i$ in (5.3) and (5.4) express the Dirac matrices acting between the spinors of nucleon $i=1,2$, i.e., in order to get the NN interaction one has to multiply the spinors $\sqrt{M_N/E_N} u_N$ of the initial and final states.

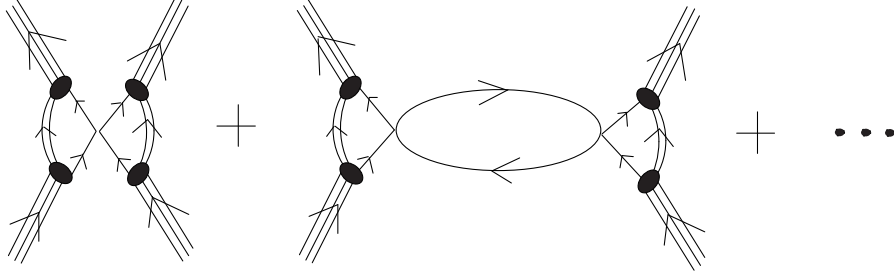


Figure 14: The NN interaction of Eq.(5.2) in the present quark-diquark model. Only those terms arising from the interaction of the two spectator quarks are shown, there are also equivalent graphs from the interaction between the quarks inside the diquarks. The term δM_σ^2 , which is included in Eq.(5.3), is not shown explicitly in this figure.

the Z-graph, we note that this is just the Pauli blocking part to the $N\bar{N}$ bubble graph, which is taken into account explicitly in the RPA series of Fig.13 and therefore should not be included in the interaction. (Numerically the Z-graph contribution is small compared to $\hat{\Pi}_\sigma$ because of the reduced σN coupling in the medium, see Ref.[11].) The self energy correction for the sigma meson arising from the induced $\bar{N}\sigma^2 N$ contact interaction is included in (5.3) as the density-dependent constant[11]

$$\delta M_\sigma^2 = 4 \left(\frac{d^2 M_N}{dM^2} \right) \int \frac{d^3 k}{(2\pi)^3} \frac{M_N}{E_N(k)} \Theta(p_F - |\mathbf{k}|). \quad (5.5)$$

The $NN\sigma$ coupling constant at zero momentum is proportional to dM_N/dM , and its square appears in (5.3). The $NN\sigma$ vertex form factor $F_\sigma(k^2)$ is normalized to $F_\sigma(0) = 1$. The first factor in (5.4) is the reduced $q\bar{q}$ t-matrix in the ω -meson channel, and the corresponding bubble graph $\hat{\Pi}_V$ is the same as in the VMD correction to the quark form factors (Fig.4). The $NN\omega$ coupling constant at zero momentum is proportional to the number of quarks in the nucleon, and the vertex form factor $F_\omega(k^2)$ is normalized as $F_\omega(0) = 1$.

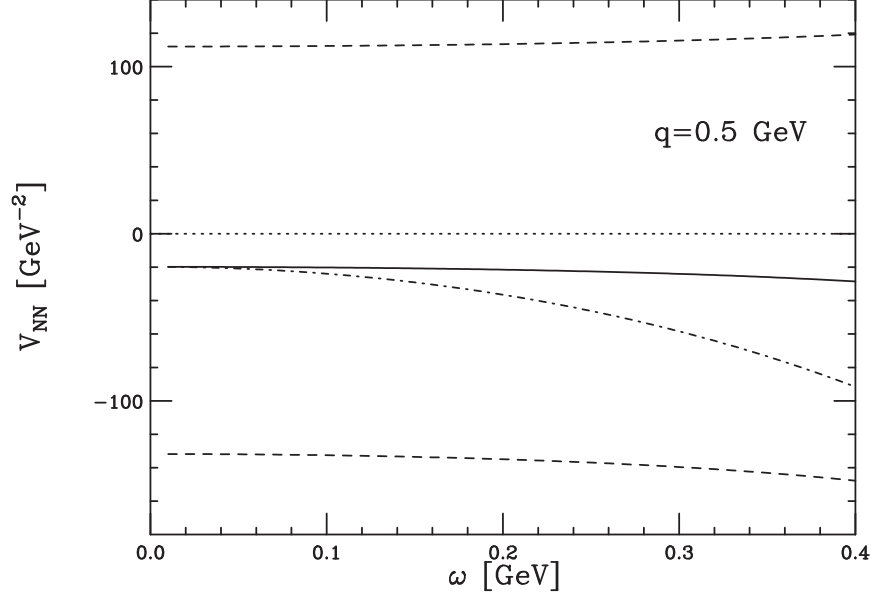


Figure 15: The NN interaction for $|\mathbf{q}| = 0.5 \text{ GeV}$ as a function of ω . The lower dashed line shows the attractive part V_σ of Eq.(5.3), the upper dashed line the repulsive piece V_ω of Eq.(5.4), the solid line shows their naive sum, and the dash-dotted line shows the combination $V_\sigma + V_\omega(1 - \omega^2/|\mathbf{q}|^2)$.

By taking matrix elements of (5.3), (5.4) between the nucleon spinors, it is easy to see that for $k = 0$ and for nucleons at the Fermi surface we just get the Landau-Migdal interaction derived more generally in Ref.([11]) (except for the Z-graph contributions as explained above). The form factor F_ω is equal to $(F_{1p} + F_{1n})$, which was calculated in the previous sections. The scalar form factor F_σ should in principle be calculated independently from the Feynman diagrams of Fig.1 by using the external operator **1**. However, because the calculations discussed below show that the RPA effects are numerically not very important, we will simply assume the same form factor as for the $NN\omega$ coupling ($F_\sigma = F_\omega$).

The two parts of the NN interaction, V_σ of (5.3) and V_ω of (5.4) , are

shown by the lower and upper dashed lines, respectively, in Fig.15 for the kinematics needed in the calculation of the response function, $|\mathbf{q}| = 0.5$ GeV and $0 < \omega < 0.4$ GeV. As in the case of relativistic hadronic models[34], we see large cancellations between the attractive scalar and repulsive vector parts. The solid line shows the naive sum of the two dashed lines, while the dash-dotted line shows the combination $V_\sigma + V_\omega(1 - \omega^2/|\mathbf{q}|^2)$, which includes the effect of the longitudinal space component of the ω exchange and is more relevant for the longitudinal response function [31]¹⁸. The results shown in Fig. 15 can be reproduced almost exactly by an approximate form in terms of Yukawa potentials, if the coupling constants and meson masses are defined at $k^2 = 0$. This is discussed in Appendix C, where also numerical values are given.

The result for the longitudinal response function of NM ($\rho = 0.16$ fm⁻³) for $|\mathbf{q}| = 0.5$ GeV is shown in Fig. 16. The dashed line is the Hartree response with the free dipole form factors, and the dash-dotted line is obtained by adding our calculated medium corrections $\Delta F(q^2; \rho) = F(q^2, \rho) - F(q^2, \rho = 0)$ to the free dipole form factors. (Here F denotes any of the Dirac-Pauli form factors.) We see that, even in this region of relatively low momentum transfers, the medium effects are appreciable. Finally, the solid line shows the result obtained by further adding the RPA corrections with the NN interaction derived above and using the density dependent meson-nucleon form factors.

We do not show a comparison to experimental data in Fig.16 because of two reasons: First, our calculation refers to NM and cannot be applied

¹⁸We have to note, however, that the true interaction in the nuclear medium in the longitudinal channel is more repulsive than shown by the dash-dotted line in Fig.15, because of the difference between the Dirac matrices $\mathbf{1}$ and γ^0 in Eq.(5.2). On the average it is repulsive on the small ω side and becomes attractive on the large ω side, as the RPA result of Fig.16 shows.

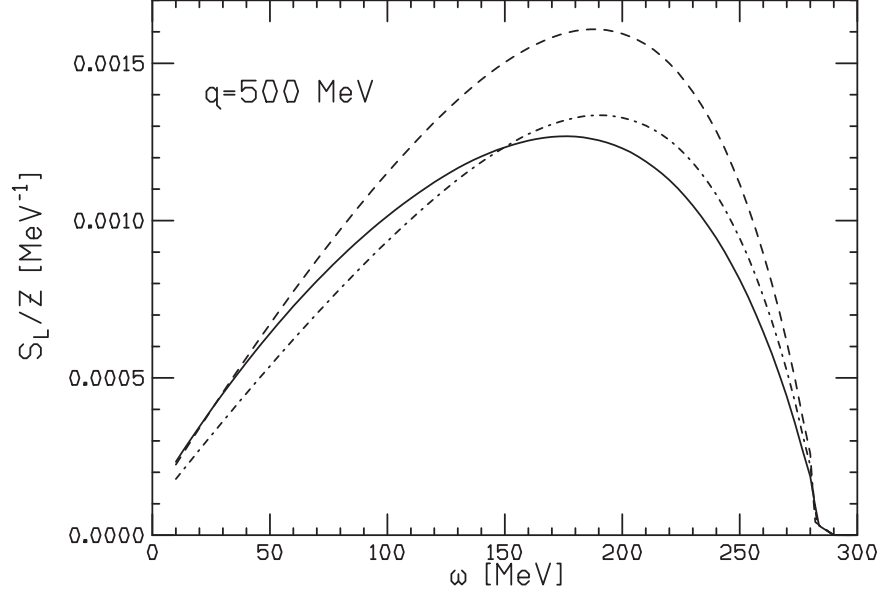


Figure 16: The longitudinal response function calculated in nuclear matter for density $\rho = 0.16 \text{ fm}^{-3}$ and $|\mathbf{q}| = 500 \text{ MeV}$ as a function of ω . Dashed line: Hartree response with free dipole form factors, dash-dotted line: Hartree response including the medium corrections to the nucleon form factors, solid line: RPA response including the medium corrections to the nucleon form factors. The NN interaction used for the RPA calculation is the one shown in Fig.15, but multiplied by meson-nucleon form factors including medium corrections as explained in the main text.

directly to finite nuclei, although for the case of ^{40}Ca the results are qualitatively very similar to the NM results, see Ref.[31]. Second, the analysis of the experimental data is still controversial, mainly because of the model dependence of the Coulomb corrections[35, 4, 36] ¹⁹.

¹⁹The analysis of Ref.[3], which did not take into account the Coulomb corrections, was refined in Ref.[4] by using a particular theoretical model for the Coulomb corrections, but it has been pointed out recently [36] that the results depend on which theoretical prescriptions are used.

6 Summary

In this paper we used a simple quark-scalar diquark picture for the single nucleon to describe the electromagnetic form factors of a nucleon bound in the nuclear medium. We used the nuclear matter equation of state derived within the same effective quark theory to assess the effect of the mean nuclear fields on the internal quark structure and the form factors of a bound nucleon, taking into account also the meson cloud around the constituent quarks. We have shown that this simple model gives reasonable results for the Dirac form factors of the free nucleon if the finite size of the diquark is taken into account. This is particularly important for the neutron in order to obtain a small F_1 , consistent with observations. Concerning the Pauli form factors, in particular the anomalous magnetic moments and the behavior for large Q^2 , one would need to further add the effect of the axial vector diquark and its finite size to achieve a reasonable description.

The medium modifications of the form factors associated with the orbital current are significant in the region of low and intermediate Q^2 , and partially associated with an increase of the electric size in the medium. The form factors associated with the spin current are enhanced because of the reduced nucleon mass, but due to a simultaneous decrease of the intrinsic anomalous magnetic moment, the total changes are not very large; in particular for the neutron they are almost zero. For both kinds of form factors - orbital and spin -, the medium modifications decrease with increasing Q^2 . This is consistent with the intuitive expectation that the mean fields, which reflect the long range nuclear correlations, should not influence the structure of the nucleon at short distances.

As an application, we considered the longitudinal response function of nuclear matter for inclusive quasielastic electron scattering. Even in this re-

gion of relatively low momentum transfer, the medium effects on the nucleon form factors give rise to an appreciable quenching of the response function. In order to take into account the RPA-type correlations between the nucleons, we derived the NN interaction in the present quark model for the isoscalar channel, which is most important for the longitudinal response function. In the limit of zero momentum transfer (Landau limit), this interaction agrees with the more general Landau-Migdal effective interaction, which was derived in earlier works for this particular quark theory, and has many features which are similar to relativistic meson-nucleon theories. In particular, it is on the average repulsive in the region below the quasielastic peak, and becomes attractive for higher energy transfers.

We finally would like to remark that the language of effective quark theories is very appropriate to address the problem of medium modifications of nucleon properties. This work represents one further step toward the goal of describing relativistic nuclear systems by taking into account the quark substructure of the constituent hadrons.

ACKNOWLEDGMENT

W.B. wishes to thank A.W. Thomas for many helpful discussions. This work was supported by the Grant in Aid for Scientific Research of the Japanese Ministry of Education, Culture, Sports, Science and Technology, Project No. C-16540267.

References

- [1] A.W. Thomas and W. Weise, *The structure of the nucleon*, Wiley-VCH, 2001.
- [2] M.K. Jones et al., Phys. Rev. Lett. **84** (2000) 1398;
O. Gayou et al., Phys. Rev. Lett. **88** (2002) 092301;
I.A. Qattan et al., Phys. Rev. Lett. **94** (2005) 142301.
- [3] Z.-E. Meziani et al., Phys. Rev. Lett. **52** (1984) 2130; **54** (1985) 1233.
- [4] C.F. Williamson et al., Phys. Rev. **C 56** (1997) 3152.
- [5] S. Dieterich et al., Phys. Lett. **B 500** (2001) 47;
S. Strauch et al., Phys. Rev. Lett. **91** (2003) 052301.,
S. Malov et al., Phys. Rev. **C 62** (2000) 057302.
- [6] D.H. Lu, K. Tsushima, A.W. Thomas, A.G. Williams and K. Saito,
Phys. Lett. **417** (1998) 217; Phys. Rev. **C 60** (1999) 068201;
J.R. Smith and G.A. Miller, Phys. Rev. **C 70** (2004) 065205;
E. Ruiz Arriola, C.V. Christov and K. Goeke, Phys. Lett. **B 225** (1989) 22.
- [7] Pre-conceptual design report on CEBAF@12 GeV
(<http://www.jlab.org>).
- [8] R. Alkofer, A. Höll, M. Kloker, A. Krassnigg and C.D. Roberts,
nucl-th/0412046;
M. Oettel and R. Alkofer, Eur. Phys. J. **A 16** (2003) 95.
- [9] R.D. Young, D.B. Leinweber and A.W. Thomas, Phys. Rev. **D 71** (2005) 014001;
H.H. Matevosyan, G. Miller and A.W. Thomas, nucl-th/0501044.

- [10] Y. Nambu and G. Jona-Lasinio, Phys. Rev. **122** (1960) 345; **124** (1961) 246.
- [11] W. Bentz and A.W. Thomas, Nucl. Phys. **A 696** (2001) 138.
- [12] H. Mineo, W. Bentz and K. Yazaki, Phys. Rev. **C 60** (1999) 065201.
- [13] H. Mineo, W. Bentz, N. Ishii, A.W. Thomas and K. Yazaki, Nucl. Phys. **A 735** (2004) 482.
- [14] I.C. Cloet, W. Bentz and A.W. Thomas, hep-ph/0504229; nucl-th/0504019.
- [15] W. Bentz, T. Horikawa, N. Ishii and A.W. Thomas, Nucl. Phys. **A 720** (2003) 95.
- [16] S. Lawley, W. Bentz and A.W. Thomas, nucl-th/0504020.
- [17] H. Mineo, W. Bentz, N. Ishii and K. Yazaki, Nucl. Phys. **A 703** (2002) 785.
- [18] W. Bentz, A. Arima and H. Baier, Nucl. Phys. **A 541** (1992) 333.
- [19] U. Vogl, W. Weise, Prog. Part. Nucl. Phys. **27** (1991) 195;
M. Buballa, hep-ph/0402234 and references therein.
- [20] N. Ishii, W. Bentz and K. Yazaki, Nucl. Phys. **A 578** (1995) 617;
M. Oettel, R. Alkofer and L. von Smekal, Eur. Phys. J. **A 8** (2000) 553.
- [21] A. Buck, R. Alkofer and H. Reinhardt, Phys. Lett. **286** (1992) 29.
- [22] D. Ebert, T. Feldmann and H. Reinhardt, Phys. Lett. **388** (1996) 154;
G. Hellstern, R. Alkofer and H. Reinhardt, Nucl. Phys. **A 625** (1997) 697.

- [23] H. Asami, N. Ishii, W. Bentz and K. Yazaki, Phys. Rev. **C 51** (1995) 3388.
- [24] M. Oettel, R. Alkofer and L.von Smekal, Eur. Phys. J. **A8** (2000) 553.
- [25] W. Bentz, L.G. Liu and A. Arima, Ann. Phys. **188** (1988) 61.
- [26] N. Isgur, Phys. Rev. Lett. **83** (1999) 272.
- [27] P. Nozieres, *Theory of interacting Fermi systems*, W.A. Benjamin, 1964;
A.B. Migdal, *Theory of finite Fermi systems*, Interscience Publishers, 1967.
- [28] A. Arima, K. Shimizu, W. Bentz and H. Hyuga, Adv. Nucl. Phys. **18** (1987) 1.
- [29] G.E. Brown, W. Weise, G. Baym and J. Speth, Comm. Nucl. Part. Phys. **17** (1987) 39;
S. Ichii, W. Bentz, A. Arima and T. Suzuki, Phys. Lett. **B 192** (1987) 11.
- [30] W. Bentz, H. Baier and A. Arima, Ann. Phys. **200** (1990) 127.
- [31] K. Tanaka, W. Bentz and A. Arima, Nucl. Phys. **A 518** (1990) 229;
K. Tanaka, W. Bentz, A. Arima and F. Beck, Nucl. Phys. **A 528** (1991) 676.
- [32] H. Kurasawa and T. Suzuki, Nucl. Phys. **A 445** (1985) 685; **A 454** (1986) 527.
- [33] K. Wehrberger and F. Beck, Phys. Rev. **C 35** (1987) 298; **C 37** (1988) 1148.
- [34] B.D. Serot and J.D. Walecka, Adv. Nucl. Phys. **16** (1986) 1.

- [35] J. Jourdan, Nucl. Phys. **A 603** (1996) 117.
- [36] J. Morgenstern and Z.-E. Meziani, Phys. Lett. **B 515** (2001) 269.

Appendices

A Expressions for the nucleon form factors

Here we give the explicit expressions for the contributions of the 3 terms in Eq.(3.11)-(3.13) to the nucleon Dirac-Pauli form factors defined in (3.14). They can be derived by invariant integration in the usual way, i.e., by (i) introducing Feynman parameters, (ii) performing a shift so that the denominator depends only on k^2 , (iii) expressing the result in the form (3.14) by using the Dirac equation for the nucleon spinors, (iv) performing a Wick rotation according to

$$-i \int \frac{d^4 k}{(2\pi)^4} f(k^2) \longrightarrow \int_0^\infty \frac{t dt}{16\pi^2} f(-t)$$

where $t = k_0^2 + \mathbf{k}^2$ is the square of the Euclidean length, and finally (v) introducing a Lorentz invariant regularization scheme, in our case the proper time regularization (2.19). Below we give the expressions which are obtained after performing the steps (i)-(iv), using $Q^2 = -q^2 > 0$ as the variable.

In the expressions given below there enter the diquark and nucleon wave function normalization factors, which are defined by (2.13) and (2.14) in terms of the renormalized bubble graphs (2.15) and (2.16), for which we have the expressions

$$\hat{\Pi}_s(p^2) = -24 \int_0^\infty \frac{t dt}{16\pi^2} \left(\frac{1}{t + M^2} + \frac{p^2}{2} \int_0^1 dx \frac{1}{(t + M^2 - p^2 x(1-x))^2} \right) \quad (\text{A.1})$$

$$\hat{\Pi}_N(p) = -\hat{g}_s \int_0^\infty \frac{t dt}{16\pi^2} \int_0^1 dx \frac{\not{p}x + M}{(t + M^2(1-x) + M_s^2 x - p^2 x(1-x))^2} \cdot \quad (\text{A.2})$$

If we denote

$$D_1(Q^2, x) = t + M^2 + Q^2 x(1-x), \quad (\text{A.3})$$

the contributions of the contact term (3.11) to the form factors are as follows:

$$\begin{aligned}
F_{1N}^{(C)}(Q^2) &= -\frac{4G_s}{\hat{g}_s} \hat{Z}_N \int_0^\infty \frac{t dt}{16\pi^2} \int_0^1 dx \\
&\times \left[F_{1Q}(Q^2) \left(\frac{1}{D_1(Q^2, x)} - \frac{1}{t+M^2} + \frac{Q^2}{2} \frac{1}{D_1(Q^2, x)^2} \right) \right. \\
&+ \left. F_{2Q}(Q^2) \frac{Q^2}{2} \frac{(1+x)(1-x\frac{M_N}{M})}{D_1(Q^2, x)^2} \right] \quad (A.4)
\end{aligned}$$

$$\begin{aligned}
F_{2N}^{(C)}(Q^2) &= \frac{4G_s}{\hat{g}_s} \hat{Z}_N M_N M \int_0^\infty \frac{t dt}{16\pi^2} \int_0^1 dx \\
&\times \left[F_{1Q}(Q^2) \frac{2}{D_1(Q^2, x)^2} + F_{2Q}(Q^2) \frac{(1-x\frac{M_N}{M})^2 - \frac{Q^2 x}{M^2}}{D_1(Q^2, x)^2} \right]. \quad (A.5)
\end{aligned}$$

If we denote

$$\begin{aligned}
D_2(Q^2, x, y) &= t + M_s^2(1-x) + M^2x - M_N^2x(1-x) + \frac{Q^2}{4}(x^2 - y^2) \\
N_1(Q^2, x) &= (M_N + M)^2 - M_s^2 - \frac{t}{2} - 2M_N^2x(1-x) - 2M_N M x \\
N_2(Q^2, x) &= \left(1 + \frac{M_N}{M}(1-x) \right)^2 - \frac{Q^2}{4M^2}(x^2 - y^2), \quad (A.6)
\end{aligned}$$

the contributions of the quark term (3.12) to the form factors are as follows:

$$\begin{aligned}
F_{1N}^{(Q)} &= \hat{Z}_N \int_0^\infty \frac{t dt}{16\pi^2} \int_0^1 dx \\
&\times \left[F_{1Q}(Q^2) \left(\frac{1}{D_1(Q^2, x)^2} + \int_{-x}^x dy \frac{N_1(Q^2, x)}{D_2(Q^2, x, y)^3} \right) \right. \\
&- \left. F_{2Q}(Q^2) \frac{Q^2}{2} \int_{-x}^x dy \frac{1 + \frac{M_N}{M}(1-x)}{D_2(Q^2, x, y)^3} \right] \quad (A.7)
\end{aligned}$$

$$\begin{aligned}
F_{2N}^{(Q)} &= \hat{Z}_N \int_0^\infty \frac{t dt}{16\pi^2} \int_0^1 dx \int_{-x}^x dy \\
&\times \left[F_{1Q}(Q^2) 2M_N x \frac{M_N(1-x) + M}{D_2(Q^2, x, y)^3} + F_{2Q}(Q^2) M_N M \frac{N_2(Q^2, x)}{D_2(Q^2, x, y)^3} \right]. \quad (A.8)
\end{aligned}$$

If we denote

$$D_3(Q^2, x, y) = t + M^2(1 - x) + M_s^2 x - M_N^2 x(1 - x) + \frac{Q^2}{4}(x^2 - y^2), \quad (\text{A.9})$$

the contributions of the diquark term (3.13) to the form factors are as follows:

$$F_{1N}^{(D)} = \hat{Z}_N F_D(Q^2) \int_0^\infty \frac{t dt}{16\pi^2} \int_0^1 dx \int_{-x}^x dy \frac{2M_N(1-x)(M_N x + M) + \frac{t}{2}}{D_3(Q^2, x, y)^3} \quad (\text{A.10})$$

$$F_{2N}^{(D)} = -\hat{Z}_N F_D(Q^2) \int_0^\infty \frac{t dt}{16\pi^2} \int_0^1 dx \int_{-x}^x dy 2M_N(1-x) \frac{M_N x + M}{D_3(Q^2, x, y)^3}. \quad (\text{A.11})$$

The diquark form factor F_D is calculated from the expression (3.16) as

$$F_D = 12\hat{g}_s \int_0^\infty \frac{t dt}{16\pi^2} \int_0^1 dx \left\{ F_{1Q}^{(0)}(Q^2) \left[\frac{1}{D_1(Q^2, x)^2} + M_s^2 \int_{-x}^x dy \frac{x}{D_4(Q^2, x, y)^3} \right] - \frac{Q^2}{2} F_{2Q}^{(0)}(Q^2) \int_{-x}^x dy \frac{1}{D_4(Q^2, x, y)^3} \right\} \quad (\text{A.12})$$

where we defined

$$D_4(Q^2, x, y) = t + M^2 - M_s^2 x(1 - x) + \frac{Q^2}{4}(x^2 - y^2), \quad (\text{A.13})$$

and $F_{1Q}^{(0)}$, $F_{2Q}^{(0)}$ are the isoscalar parts of the quark form factors.

B Expressions for the quark form factors

Here we give the expressions for the quark electromagnetic vertex (3.25) in terms of the quark form factors defined in Eq.(3.8). In the expressions given below there enter the pion and quark wave function normalizations \hat{g}_π and \hat{Z}_Q , which are defined in terms of the renormalized self energies $\hat{\Pi}_\pi$ and $\hat{\Sigma}_Q$ by Eqs. (3.24) and (3.26). The expression for $\hat{\Pi}_\pi = \hat{\Pi}_s$ has been given in

Eq.(A.1), and

$$\hat{\Sigma}_Q(p) = -3\hat{g}_\pi \int_0^\infty \frac{t dt}{16\pi^2} \int_0^1 dx \frac{\not{p}x - M}{(t + M^2(1-x) + M_\pi^2 x - p^2 x(1-x))^2} \quad (\text{B.1})$$

As explained in the main text, the isoscalar (or isovector) parts of the quark vertices given below should eventually be further multiplied by the VMD form factors (3.32), where the expression for $\hat{\Pi}_V$ is

$$\hat{\Pi}_V(Q^2) = 48 Q^2 \int_0^\infty \frac{t dt}{16\pi^2} \int_0^1 dx \frac{x(1-x)}{D_1(Q^2, x)^2}. \quad (\text{B.2})$$

The quark diagram (second term in (3.25)) gives the following contributions to the quark form factors:

$$F_{1Q}^{(Q)} = \frac{1}{2} (1 - \tau_3) \hat{g}_\pi \int_0^\infty \frac{t dt}{16\pi^2} \int_0^1 dx \left[\frac{1}{D_1(Q^2, x)^2} + \int_{-x}^x dy \frac{2M^2 x^2 - M_\pi^2 - \frac{t}{2}}{D_5(Q^2, x, y)^3} \right] \quad (\text{B.3})$$

$$F_{2Q}^{(Q)} = -\frac{1}{2} (1 - \tau_3) \hat{g}_\pi \int_0^\infty \frac{t dt}{16\pi^2} \int_0^1 dx \int_{-x}^x dy \frac{2M^2 x^2}{D_5(Q^2, x, y)^3} \quad (\text{B.4})$$

where

$$D_5(Q^2, x, y) = t + M_\pi^2(1-x) + M^2 x^2 + \frac{Q^2}{4}(x^2 - y^2). \quad (\text{B.5})$$

The pion diagram (third term in (3.25)) gives the following contributions to the quark form factors:

$$F_{1Q}^{(\pi)} = -2\tau_3 \hat{g}_\pi F_\pi(q^2) \int_0^\infty \frac{t dt}{16\pi^2} \int_0^1 dx \int_{-x}^x dy \frac{2M^2(1-x)^2 - \frac{t}{2}}{D_6(Q^2, x, y)^3} \quad (\text{B.6})$$

$$F_{2Q}^{(\pi)} = 4\tau_3 M^2 \hat{g}_\pi F_\pi(q^2) \int_0^\infty \frac{t dt}{16\pi^2} \int_0^1 dx \int_{-x}^x dy \frac{(1-x)^2}{D_6(Q^2, x, y)^3}, \quad (\text{B.7})$$

where

$$D_6(Q^2, x, y) = t + M^2(1-x)^2 + M_\pi^2 x + \frac{Q^2}{4}(x^2 - y^2). \quad (\text{B.8})$$

The pion form factor is calculated from (3.23) and (3.28) as

$$F_\pi = 12\hat{g}_\pi \int_0^\infty \frac{tdt}{16\pi^2} \int_0^1 dx \left[\frac{1}{D_1(Q^2, x)^2} + M_\pi^2 \int_{-x}^x dy \frac{x}{D_7(Q^2, x, y)^3} \right], \quad (\text{B.9})$$

where

$$D_7(Q^2, x, y) = t + M^2 - M_\pi^2 x(1-x) + \frac{Q^2}{4}(x^2 - y^2). \quad (\text{B.10})$$

C The NN interaction

Here we provide some details on the NN interaction Eqs.(5.2).

The bubble graph in the sigma channel, which appears in (5.3), has the form

$$\begin{aligned} \hat{\Pi}_\sigma(k^2) &= 6i \int \frac{d^4q}{(2\pi)^4} \text{Tr}_D (S_F(q) S_F(k+q)) \\ &= 12 \int_0^\infty \frac{tdt}{16\pi^2} \left[\frac{2}{t+M^2} + (k^2 - 4M^2) \int_0^1 dx \frac{1}{(t+M^2 - k^2x(1-x))^2} \right]. \end{aligned} \quad (\text{C.1})$$

The expression for $\hat{\Pi}_V$ has been given in (B.2).

In the calculations of Sect.5, the NN interaction (5.2) is used without further approximations. Here we wish to give an approximate form in terms of Yukawa potentials: Expanding $\hat{\Pi}_\sigma$ and $\hat{\Pi}_V$ around $k^2 = 0$, we obtain

$$V_{\text{NN}}(k) = \frac{g_{\sigma N}}{k^2 - M_\sigma^2} (\mathbf{1}) \cdot (\mathbf{1}) - \frac{g_{\omega N}}{k^2 - M_\omega^2} (\gamma_\mu) \cdot (\gamma^\mu), \quad (\text{C.2})$$

where

$$g_{\sigma N} = \left(\frac{dM_N}{dM} \right)^2 g_\sigma = (2.34)^2 \times 21.75 = 119.4 \quad (\text{C.3})$$

$$g_{\omega N} = 9 g_\omega = 9 \times 18.43 = 165.9, \quad (\text{C.4})$$

where the quark-meson couplings are defined by

$g_\sigma = \left[\left(\partial \hat{\Pi}_\sigma / \partial k^2 \right)_{k^2=0} \right]^{-1}$ and $g_\omega = \left[- \left(\partial \hat{\Pi}_V / \partial k^2 \right)_{k^2=0} \right]^{-1}$, and the numerical values given above are obtained from our nuclear matter EOS for $\rho = 0.16 \text{ fm}^{-3}$. The meson masses defined at zero momentum are

$$M_\sigma^2 = g_\sigma \left(\frac{1}{2G_\pi} - \hat{\Pi}_\sigma(0) + \delta M_\sigma^2 \right) = (0.81 \text{ GeV})^2 \quad (\text{C.5})$$

$$M_\omega^2 = \frac{g_\omega}{2G_\omega} = (1.13 \text{ GeV})^2. \quad (\text{C.6})$$

Note that these masses are different from the pole positions.